ELSEVIER

Journal of Biomechanics 38 (2005) 667–672

JOURNAL OF BIOMECHANICS

www.elsevier.com/locate/jbiomech
www.JBiomech.com

ASB Microstrain Award

Depth-dependent strain of patellofemoral articular cartilage in unconfined compression

Oliver K. Erne[a], John B. Reid[b], Larry W. Ehmke[a], Mark B. Sommers[a], Steven M. Madey[a], Michael Bottlang[a,*]

[a] *Biomechanics Laboratory, Legacy Clinical Research & Technology Center, 1225 NE 2nd Avenue, Portland, OR 97232, USA*
[b] *Department of Orthopaedics and Rehabilitation, Oregon Health & Science University, Portland, OR, USA*

Accepted 4 April 2004

Abstract

This biomechanical study reports strain gradients in patellofemoral joint cross-sections of seven porcine specimens in response to 1% unconfined axial compression subsequent to specific amounts of off-set strain. Strain distributions were quantified with a customized laser-based electronic speckle pattern interferometry (ESPI) system in a non-contact manner, delivering high-resolution, high-sensitivity strain maps over entire patellofemoral cartilage cross-sections.

Strain reports were evaluated to determine differences in strain magnitudes between the superficial, middle, and deep cartilage layers in femoral and patellar cartilage. In addition, the effect of 5%, 10%, 15%, and 20% off-set strain on depth-dependent strain gradients was quantified. Regardless of the amount of off-set strain, the superficial layer of femoral cartilage absorbed the most strain, and the deep layer absorbed the least strain. These depth-dependent strain gradients were most pronounced for 5% off-set strain, at which the superficial layer absorbed on average 5.7 and 23.7 times more strain as compared to the middle and deep layers, respectively. For increased off-set strain levels, strain gradients became less pronounced. At 20% off-set strain, differences in layer-specific strain were not statistically significant, with the superficial layer showing a 1.4 fold higher strain as the deep layer. Patellar cartilage exhibited similar strain gradients and effects of off-set strain, although the patellar strain was on average 19% larger as compared to corresponding femoral strain reports.

This study quantified for the first time continuous strain gradients over patellofemoral cartilage cross-sections. Next to provision of a detailed functional characterization of normal diarthrodial joints, this novel experimental approach holds considerable attraction to investigate joint degenerative processes.

Keywords: Articular cartilage; Compression; Strain measurement; Patellofemoral joint

1. Introduction

Articular cartilage of diarthrodial joints is a complex composite, which can provide load distribution, impact damping, and low-friction sliding under demanding loading conditions throughout an entire live-span (Mow et al., 1984; Lai et al., 1991; Buckwalter, 2002). Detailed characterization of the mechanical properties of articular cartilage is an essential prerequisite to investigate degenerative processes and to engineer interventions for cartilage repair. This research introduced a novel laser-based measurement approach capable of characterizing strain distributions over patellofemoral cartilage cross-sections with unprecedented sensitivity.

Classical compression tests, utilizing unconfined compression, indentation, and confined compression on full-thickness cartilage samples have been invaluable tools to determine material properties of nonlinear viscoelastic, anisotropic, and multi-phasic articular cartilage for a wide range of cartilage conditions and loading regimes (Hayes and Mockros, 1971; Suh and Spilker, 1994; Bursac et al., 1999; DiSilvestro and Suh, 2001). However, test results were limited to bulk properties averaged over the test specimen volume. Recognizing the dramatic differences in collagen fiber

*Corresponding author. Tel.: +503-413-5457; fax: +503-413-5216.
E-mail address: mbottlan@lhs.org (M. Bottlang).

0021-9290/$ - see front matter © 2004 Elsevier Ltd. All rights reserved.
doi:10.1016/j.jbiomech.2004.04.005

orientation and proteoglycan concentration between specific cartilage regions, compression tests of partial-thickness cartilage samples have been conducted (Mow et al., 1984; Flachsmann et al., 2001; Chen et al., 2001). These tests yielded characteristic differences in mechanical properties between cartilage samples, harvested from surface, middle and deep cartilage layers.

Driven by the apparent implications of these characteristic differences in layer-specific cartilage properties for cartilage function, a multitude of experimental approaches have been employed to quantify layer-specific properties in full-thickness cartilage samples (Clark et al., 2003; Guilak et al., 1995; Schinagl et al., 1996, 1997; Wang et al., 2003). Guilak et al. (1995) used confocal microscopy to measure chondrocyte deformation over cartilage cross-sections to infer depth-dependent cartilage strain under quasi-static loading. Microscopic approaches enabled tracing of cartilage deformation and strain with high spatial resolution, but necessarily confined the region of observation to the microscopic range. Alternatively, high-resolution macroscopic imaging techniques in combination with image correlation algorithms have been used to acquire the inhomogeneous deformation and strain response over entire cartilage cross-sections (Schinagl et al., 1996; Wang et al., 2003). Schinagl et al. (1996) used chondrocyte nuclei as fiduciary markers and traced their displacement in cartilage cross-sections in response to incremental amounts of confined compression. However, these full-field techniques are lacking the resolution of the microscopic studies.

This study employed for the first time a laser-based strain measurement technique (electronic speckle pattern interferometry ESPI), which allows to capture full-field strain maps over entire patellofemoral cartilage cross-sections with high sensitivity and spatial resolution. The objectives of the present study were quantification of strain gradients in articular cartilage; and determining changes thereof in response to various amounts of cartilage compression.

2. Materials and methods

2.1. Specimens

Seven specimens each were harvested from the trochlear region of medial femoral condyles and from corresponding locations on medial patellar facets of fresh frozen porcine knees. Specimens were excised perpendicular to the articular surface in shape of cubic columns of 5 mm × 5 mm × 7 mm size, using a diamond saw. Each specimen contained full-thickness cartilage and subchondral bone, and was indexed to preserve specimen orientation (Fig. 1a). Until the day of testing, specimens remained submersed in physiologic saline and frozen at −30°C. At the day of testing, specimens were thawed and stained with hematoxylin and eosin to ensure adequate surface reflective properties for strain measurement.

2.2. Experimental setup

A custom-designed compression stage was built to subject corresponding pairs of osteochondral specimens to unconfined uniaxial compression in displacement control (Fig. 1b). The subchondral bone of femoral specimens was rigidly affixed to a stationary clamp. Corresponding patellar specimens were affixed to a precision displacement stage (M-462-XM, Newport, Irvine, CA) in a manner to maximize congruency between adjacent cartilage surfaces. Each side of the articular cartilage specimen remained unconfined, and was immersed in physiologic saline. A glass plate was suspended 1 mm above the patellofemoral specimen to allow for optical strain assessment on cartilage cross-sections through a defined and stable fluid-solid interface. Cartilage compression was manually applied with a precision micrometer (DS-4F, Newport, Irvine, CA) acting upon the translation stage. The resulting displacement was acquired by a displacement transducer (LVDT, LD 400-5, Omega, Stamford, CT) with 0.1 μm

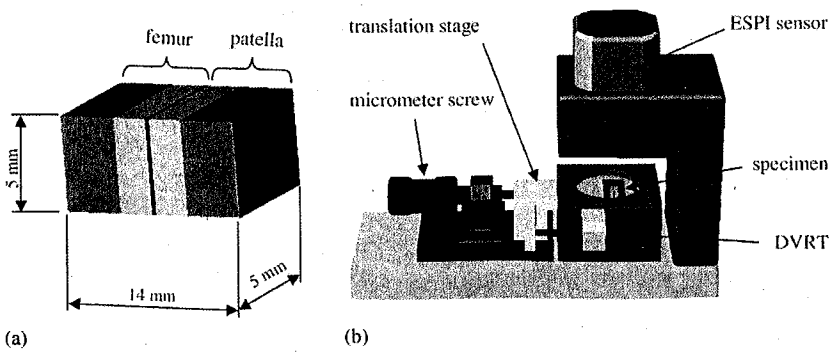

Fig. 1. (a) Patellofemoral porcine specimen; (b) experimental setup for unconfined compression of specimens and strain assessment with ESPI sensor.

resolution. Displacement reports were divided in real-time by the initial cartilage thickness to continuously monitor the applied compressive strain ε_A over the entire specimen.

2.3. Strain acquisition

A state-of-the-art ESPI sensor (Q100, Ettemeyer AG, Nersingen, Germany) was suspended over the specimens to obtain full-field displacement and strain reports over a region of interest (ROI) which spanned the entire patellofemoral cartilage cross-section and the adjacent subchondral bone regions. This laser-based non-contact measurement system generated laser speckle images of the specimen surfaces before and after cartilage compression. Subsequent speckle image subtraction and fringe analysis algorithms (ISTRA Q100 V2.7, Ettemeyer AG, Nersingen, Germany) enabled quantification of surface displacement in absence of specific surface markers. The ESPI system sequentially captured speckle images from three linear independent illumination directions to allow for computation of surface displacement vectors. In combination with custom-built magnification optics, it acquired three-directional displacement reports at 256×256 individual locations over a $10\,\text{mm} \times 8\,\text{mm}$ ROI. Next to delivering a continuous outcome array over a macroscopic measurement range, the ESPI system captured surface displacement at a resolution of $<80\,\text{nm}$ ($\approx 1/10$ of laser wave length). Due to this high measurement resolution, individual ESPI measurements were limited to surface deformations of $<1\,\mu\text{m}$. To capture larger deformations in cartilage specimens, sequential ESPI recordings over a series of small incremental cartilage compression steps were required. Surface displacement reports were differentiated in direction perpendicular to the articular surface to yield the compressive strain distributions over the ROI. These strain results, based on $40\,\mu\text{m}$ gage length, were subsequently smoothed by non-weighted, moving box-car averaging with a $200\,\mu\text{m}$ array width.

2.4. Strain application and evaluation

Specimens were gradually compressed to off-set strains of $\varepsilon_O = 5\%$, 10%, 15% and 20% (Fig. 2). At each of these four off-set strain levels, specimens were allowed to equilibrate for 1 h. After equilibration at each off-set strain level, specimens were subjected to a series of small incremental compression steps up to a total additional compression of $\Delta\varepsilon = 1\%$. After each incremental compression step, ESPI recordings were obtained. Serial ESPI recordings were evaluated to obtain full-field strain distributions ε_{5-6}, ε_{10-11}, ε_{15-16}, and ε_{20-21}, reflecting changes in strain distribution due to 1% incremental loading after off-set strain application of 5%, 10%, 15%, and 20%, respectively. Subsequently,

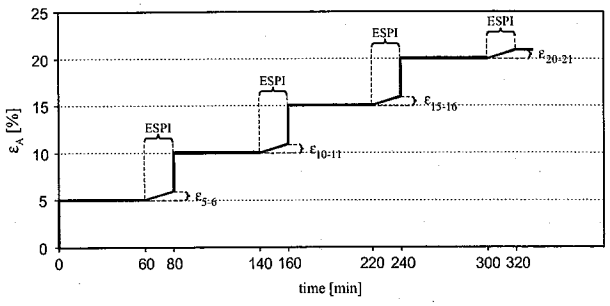

Fig. 2. Loading regime for unconfined compression of specimens by 1% subsequent to 5%, 10%, 15%, and 20% off-set strain and 60 min equilibration intervals.

these full-field strain distributions were reduced by averaging all strain reports obtained at a given cartilage depth to extract strain profiles over cartilage cross-sections in response to 1% incremental loading for the four distinct off-set strain levels. These strain profiles were further reduced by averaging strain values over specific cartilage layers (Mow et al., 1984) to extract the superficial layer strain ε_S (0–20% of cartilage depth), middle layer strain ε_M (21–70% depth), and deep layer strain ε_D (71–100% depth), individually for the femoral and patellar cartilage. Differences between layer-specific strains ε_S, ε_M, ε_D for a given off-set strain amount were statistically analyzed by two-tailed, unpaired, Student's t-tests. Variances in outcome parameters were denoted by ± 1 standard deviation.

3. Results

The ESPI sensor obtained full-field deformation and strain maps over entire patellofemoral cartilage cross-sections in response to incremental compression of $\Delta\varepsilon = 1\%$ (Fig. 3a). Repeatability of ESPI strain reports was assessed in terms of strain profiles obtained over the cross-section of one specimen, subjected three times to $\Delta\varepsilon = 1\%$ at 5% off-set strain. Resulting strain profiles and associated peak strain magnitudes ($4.6\% \pm 0.21\%$) were highly repeatable (Fig. 3b).

Articular cartilage specimens exhibited distinct depth-dependent strain distributions in response to uniaxial compression $\Delta\varepsilon = 1\%$. These strain gradients were most pronounced at 5% off-set strain (Fig. 4). Strain gradients between cartilage layers gradually decreased with an increase in off-set strain. In femoral cartilage under 5% off-set strain, the superficial layer strain ε_S was significantly higher ($p<0.01$) as compared to the mid- and deep-layer strain ε_M and ε_D (Fig. 5). On average, ε_S ($2.3\% \pm 1.2\%$) was 5.7 and 23.7 times larger as compared to ε_M ($0.39\% \pm 0.54\%$) and ε_D ($0.09\% \pm 0.06\%$), respectively. For off-set-strains of 10%, 15%, and 20%, ε_S was on average 7.3, 2.9, and 1.4 times larger

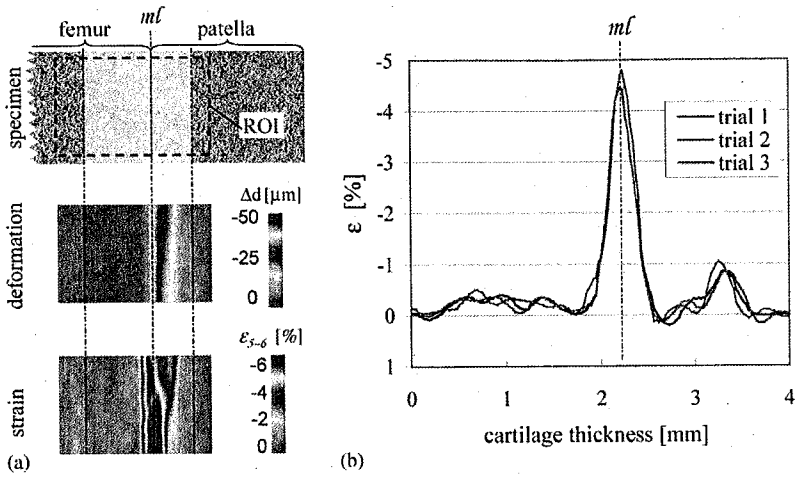

Fig. 3. (a) Deformation and strain across patellofemoral cartilage in response to $\Delta\varepsilon = 1\%$; (b) repeatability evaluation of three ESPI strain measurements on one representative specimen, based on strain gradients extracted from full-field strain maps.

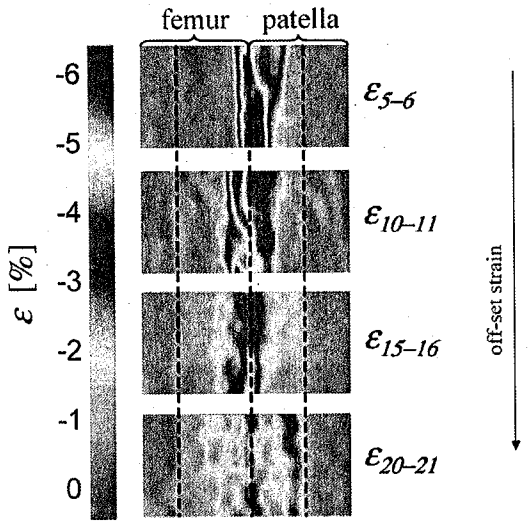

Fig. 4. ESPI reports of strain gradients across patellofemoral specimens in response to 1% incremental compression subsequent to 5%, 10%, 15%, and 20% off-set strain.

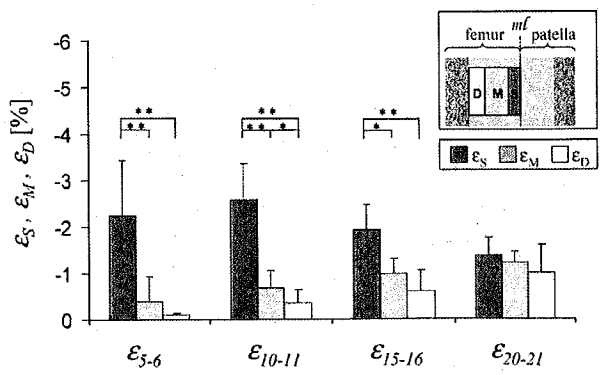

Fig. 5. Femoral cartilage strain gradients: depth-dependent strain magnitudes in superficial, medial, and deep cartilage layers in response to 1% compression for four specific off-set strain levels.

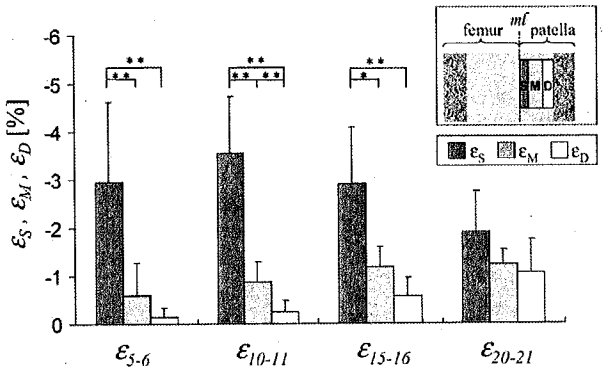

Fig. 6. Patellar cartilage strain gradients: depth-dependent strain magnitudes in superficial, medial, and deep cartilage layers in response to 1% compression for four specific off-set strain levels.

as compared to ε_D, respectively. At 20% off-set strain, differences between ε_S, ε_M, and ε_D were not statistically significant.

In patellar cartilage under 5% off-set strain, the superficial layer exhibited significantly higher strain as compared to the middle and deep layer ($p < 0.01$) (Fig. 6). On average, ε_S ($3.0\% \pm 1.7\%$) was 5.0 and 20.1 times larger as compared to ε_M ($0.59\% \pm 0.66\%$) and ε_D ($0.15\% \pm 0.18\%$), respectively. As previously observed in femoral cartilage, strain gradients between patellar cartilage layers gradually decreased with an increase in off-set strain. For off-set-strains of 10%, 15%, and 20%, ε_S was on average 4.1, 2.5, and 1.6 times larger as compared to ε_D, respectively. At 20% off-set strain, differences between ε_S, ε_M, and ε_D were not statistically significant.

Strain in response to incremental compression of $\Delta\varepsilon = 1\%$ was not equally distributed between femoral and patellar cartilage, with the patellar cartilage absorbing the majority of strain. In comparison to the

femoral cartilage, patellar cartilage absorbed 28%, 21%, 18%, and 8.3% more strain for off-set strain levels of 5%, 10%, 15% and 20%, respectively.

4. Discussion

Results of the present study describe strain gradients over articular cartilage cross-sections as a function of off-set strain. Furthermore, we were able to correlate strain gradients on opposing sides of corresponding portions of patellofemoral cartilage.

Observed depth-dependent strain gradients correlate to findings of Guilak et al. (1995). They used confocal microscopy to measure the degree of chondrocyte deformation in the superficial, middle, and deep layers of canine femoral cartilage. When full-thickness explants were compressed to 15% surface-to-surface strain, a 19.1% deformation of superficial chondrocytes was observed compared to 14.8% and 15.7% for the middle and deep zones, respectively. The authors concluded that the compressive stiffness of articular cartilage was greater in the middle and deep zones when compared with the superficial zone. This agrees with results of the present study, which demonstrated in both, the patellar and femoral cartilage that strain was significantly larger in the superficial layer when compared with the middle and deep layers. This difference, however, decreased with increasing off-set strain. This finding supports the pattern observed in past research that utilized fluorescently labeled chondrocyte nuclei to study the effect of progressive compressive deformation. Schinagl et al. (1997) compressed osteochondral samples by 8%, 16%, 24%, and 32% of the articular thickness and used the position of chondrocyte nuclei to assess depth-dependent cartilage strain. Small amounts of compression resulted primarily in superficial zone strain, while little deformation was observed in the deep zone. However, with increasing levels of compression, strain increased more evenly in all cartilage zones. This effect may be explained by increased extrusion of the fluid phase from the solid matrix in response to increasing amounts of cartilage compression. Under these quasi-static, unconfined loading conditions, increased compression will therefore progressively shift load bearing from the fluid phase to the solid matrix.

This effect was observed in the patellar and the femoral specimens. At all off-set strain levels, strain gradients over the three cartilage zones were similar between patellar and femoral specimens. However, the strain magnitude was greater in patellar specimens as compared to femoral specimens by an average of 19%. This observation correlates to recent data obtained using chondrocyte deformation to study feline patellofemoral compression (Clark et al., 2003). They found that at 9 and 15 MPa the femoral groove experienced 18% and 30% less strain than the corresponding patellar tissue, respectively. Previously, Herberhold et al. (1999) found a similar trend using magnetic resonance imaging to study patellofemoral deformation of a pneumatically loaded knee joint. Under 1.5 times body-weight loading, the decrease in thickness of the patellar articular cartilage was on average 32% greater as compared to the femoral cartilage. These reports furthermore correlate to indentation test results of Froimson et al. (1997) who found the compressive modulus of the patellar articular cartilage to be 30% lower as compared to femoral cartilage.

Employment of non-contact, full-field ESPI technology enabled functional characterization of articular cartilage in great detail. ESPI offered the unique ability to capture strain with high sensitivity and high spatial resolution over entire patellofemoral cartilage cross-sections. This allowed quantification of subtle yet distinct mechanisms of cartilage function. As such, the experimental approach holds strong potential to study normal cartilage function and degenerative changes thereof in a quantitative approach. However, this experimental approach is limited to quasi-static measurements and visual access to the measurement area. This in turn required in situ loading of cartilage explants in unconfined compression. Furthermore, results obtained on porcine specimens can not directly be correlated to human articular cartilage (Athanasiou et al., 1991).

Acknowledgements

Financial assistance was provided by a grant from the Legacy Research Foundation.

References

Athanasiou, K.A., Rosenwasser, M.P., Buckwalter, J.A., Malinin, T.I., Mow, V.C., 1991. Interspecies comparisons of in situ intrinsic mechanical properties of distal femoral cartilage. Journal of Orthopaedic Research 9, 330–340.

Buckwalter, J.A., 2002. Articular cartilage injuries. Clinical Orthopaedics and Related Research 402, 21–37.

Bursac, P.M., Obitz, T.W., Eisenberg, S.R., Stamenovic, D., 1999. Confined and unconfined stress relaxation of cartilage: appropriateness of a transversely isotropic analysis. Journal of Biomechanics 32, 1125–1130.

Chen, A.C., Bae, W.C., Schinagl, R.L., Sah, R.L., 2001. Depth and strain-dependent mechanical and electromechanical properties of full-thickness bovine articular cartilage in confined compression. Journal of Biomechanics 34, 1–12.

Clark, A.L., Barclay, L.D., Matyas, J.R., Herzog, W., 2003. In situ chondrocyte deformation with physiological compression of the feline patellofemoral joint. Journal of Biomechanics 36, 553–568.

DiSilvestro, M.R., Suh, J.K., 2001. A cross-validation of the biphasic poroviscoelastic model of articular cartilage in unconfined compression, indentation, and confined compression. Journal of Biomechanics 34, 519–525.

Flachsmann, R., Broom, N.D., Hardy, A.E., 2001. Deformation and rupture of the articular surface under dynamic and static compression. Journal of Orthopaedic Research 19, 1131–1139.

Froimson, M.I., Ratcliffe, A., Gardner, T.R., Mow, V.C., 1997. Differences in patellofemoral joint cartilage material properties and their significance to the etiology of cartilage surface fibrillation. Osteoarthritis Cartilage 5 (6), 377–386.

Guilak, F., Ratcliffe, A., Mow, V.C., 1995. Chondrocyte deformation and local tissue strain in articular cartilage: a confocal microscopy study. Journal of Orthopaedic Research 13, 410–421.

Hayes, W.C., Mockros, L.F., 1971. Viscoelastic properties of human articular cartilage. Journal of Applied Physiology 31 (4), 562–568.

Herberhold, C., Faber, S., Stammberger, T., Steinlechner, M., Putz, R., Englmeier, K.H., Reiser, M., Eckstein, F., 1999. In situ measurement of articular cartilage deformation in intact patellofemoral joints under static loading. Journal of Biomechanics 32, 1287–1295.

Lai, W.M., Hou, J.S., Mow, V.C., 1991. A triphasic theory for the swelling and deformation behaviors of articular cartilage. Journal of Biomechanical Engineering 113, 245–258.

Mow, V.C., Holmes, M.H., Lai, W.M., 1984. Fluid transport and mechanical properties of articular cartilage: a review. Journal of Biomechanics 17 (5), 377–394.

Schinagl, R.M., Ting, M.K., Price, J.H., Sah, R.L., 1996. Video microscopy to quantitate the inhomogeneous equilibrium strain within articular cartilage during confined compression. Annals of Biomedical Engineering 24, 500–512.

Schinagl, R.M., Gurski, D., Chen, A.C., Sah, R.L., 1997. Depth-dependent confined compressive modulus of full-thickness bovine articular cartilage. Journal of Orthopaedic Research 15 (4), 499–506.

Suh, J.K., Spilker, R.L., 1994. Indentation analysis of biphasic articular cartilage: nonlinear phenomena under finite deformation. Journal of Biomechanical Engineering 116, 1–9.

Wang, C.C.B., Chahine, N.O., Hung, C.T., Ateshian, G.A., 2003. Optical determination of anisotropic material properties of bovine articular cartilage in compression. Journal of Biomechanics 36, 339–353.